

The Role of the Coordination Modes of a Flexible Bis(pyridylamide) Ligand in the Topology of 2D Copper(II) Complexes

Xiu-Li Wang, Peng Liu, Jian Luan, Hong-Yan Lin, and Chuang Xu

Department of Chemistry, Bohai University, Jinzhou, 121000, P. R. China

Reprint requests to Prof. Xiu-Li Wang. E-mail: wangxiuli@bhu.edu.cn

Z. Naturforsch. **2012**, 67b, 877–886 / DOI: 10.5560/ZNB.2012-0179

Received July 2, 2012

Two new two-dimensional copper(II) coordination polymers, $[\text{Cu}(\text{L})(\text{BDC})]\cdot\text{H}_2\text{O}$ (**1**) and $[\text{Cu}_2(\text{L})_{0.5}(\text{SIP})(\text{OH})(\text{H}_2\text{O})]\cdot 2\text{H}_2\text{O}$ (**2**) [$\text{L} = N,N'$ -bis(3-pyridylamide)-1,6-hexane, $\text{H}_2\text{BDC} = 1,3$ -benzenedicarboxylic acid, $\text{H}_3\text{SIP} = 5$ -sulfoisophthalic acid (3,5-dicarboxybenzenesulfonic acid)], have been synthesized hydrothermally by self-assembly of the flexible bis-pyridyl-bis-amide ligand **L** and the aromatic polycarboxylate ligands H_2BDC or H_3SIP . X-Ray diffraction analysis reveals that complex **1** displays a metal-organic coordination layer with a binodal (3,5)-connected $\{4^2.6^7.8\}\{4^2.6\}$ topology, in which the **L** ligands adopt a μ_2 -bridging mode (*via* ligation of the pyridyl nitrogen atoms). Complex **2** also exhibits a layered network based on tetranuclear copper clusters $[\text{Cu}_4(\mu_3\text{-OH})_2(\text{H}_2\text{O})_2(\text{O}_2\text{C})_4]$, **L** ligands and **SIP** anions, showing a binodal (4,8)-connected network with $\{4^{14}.6^{10}.8^4\}\{4^4.6^2\}$ topology, in which the **L** ligands adopt a μ_6 -bridging coordination mode (*via* ligation of the pyridyl nitrogen and carbonyl oxygen atoms). Adjacent layers in **1** and **2** are further linked by hydrogen bonding interactions to form three-dimensional supramolecular frameworks. The electrochemical behavior of the two complexes in bulk-modified carbon paste electrodes has been investigated.

Key words: Flexible Bis-pyridyl-bis-amide Ligand, Copper(II) Complexes, Crystal Structures, Topologies, Electrochemical Behavior

Introduction

The construction of metal-organic coordination complexes has attracted considerable attention in the field of crystal engineering and materials chemistry, stemming from their fascinating architectures and potential applications in host-guest chemistry, catalysis, luminescence, and magnetism [1–4]. The proper selection of organic ligands is a key factor because deliberate structural changes of the organic building blocks such as length, flexibility and symmetry can dramatically change the final structures of the complexes. A large number of coordination complexes with various structures have been prepared based on rigid, linear bipyridyl ligands [5–12]. However, to our knowledge, the use of flexible bipyridyl ligands showing conformational freedom was less explored [13–17].

Recently, using the rigid bis-pyridyl-bis-amide ligand 4-bpcb [4-bpcb = N,N' -bis(4-pyridylamide)-1,4-benzene], we have obtained a novel three-dimensional metal-organic coordination polymer

$[\text{Cu}_3(4\text{-bpcb})_3(\text{BTC})_2]_3 \cdot \sim 12\text{H}_2\text{O}$, in which discrete $(\text{H}_2\text{O})_{12}$ clusters are dispersed in the three-fold interpenetrating 3D metal-organic framework [18]. With the semi-rigid isomeric bipyridyl ligands bis(3-pyridylformyl)piperazine (3-bpfp) and bis(4-pyridylformyl)piperazine (4-bpfp) and with aromatic polycarboxylate ligands 1,3- H_2BDC (1,3- $\text{H}_2\text{BDC} = 1,3$ -benzenedicarboxylic acid) or 1,3,5- H_3BTC (1,3,5- $\text{H}_3\text{BTC} = 1,3,5$ -benzenetricarboxylic acid) as the bridging ligands, our group has obtained two layered structures and a novel 3,5-connected binodal 3D topology [19]. As an extension of our study, we prepared the bipyridyl ligand N,N' -bis(3-pyridinecarboxamide)-1,6-hexane (**L**) containing a flexible bridging group. Its backbone $-(\text{CH}_2)_6-$ can be bent to satisfy the coordination requirements of metal centers, and the amide groups can provide additional coordination sites, which may lead to intriguing complexes and novel structure topologies. Additionally, the **L** ligand has heteroatoms as hydrogen-bonding acceptors, which may further

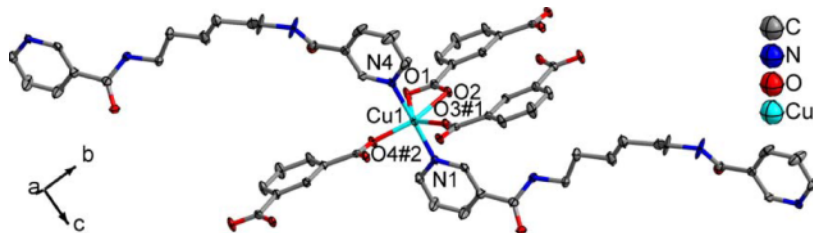


Fig. 1 (color online). The coordination environment for the Cu(II) ion in complex **1** (ellipsoids at the 50% probability level). All H atoms and lattice water molecules are omitted for clarity.

affect the final structures and the properties of the complexes.

In this paper, we report the synthesis of two new 2D copper(II) coordination polymers $[\text{Cu}(\text{L})(\text{BDC})]\cdot\text{H}_2\text{O}$ (**1**) and $[\text{Cu}_2(\text{L})_{0.5}(\text{SIP})(\text{OH})(\text{H}_2\text{O})]\cdot 2\text{H}_2\text{O}$ (**2**) with **L** as the main linker and BDC or SIP as auxiliary ligands [H_3SIP = 5-sulfoisophthalic acid (3,5-dicarboxybenzenesulfonic acid)]. Their thermal stability and electrochemical properties in bulk-modified carbon paste electrodes (CPEs) have been examined.

Results and Discussion

Complex **1** was synthesized hydrothermally in ~31% yield based on Cu. Crystals were washed with water and dried in air. Likewise, complex **2** was synthesized in a hydrothermal reaction in ~25% yield based on Cu.

Crystal and molecular structure of $[\text{Cu}(\text{L})(\text{BDC})]\cdot\text{H}_2\text{O}$ (**1**)

Single-crystal X-ray analysis has shown that complex **1** is a layer polymer based on **L** and BDC as bridging ligands. The coordination environment of the Cu(II) ion is shown in Fig. 1. The Cu1 ion is coordinated by four carboxyl oxygen atoms from three BDC ligands with Cu–O distances of 1.960(2)–2.533(3) Å, and two nitrogen atoms from two **L** ligands with Cu–N distances of 2.011(3) (Cu1–N1) and 2.016(3) Å (Cu1–N4), showing a distorted octahedral geometry. Both carboxyl groups of the BDC ligand are deprotonated and show two different coordination modes: a bidentate bridging mode and a chelating mode. Each BDC ligand links three adjacent Cu(II) ions to construct a neutral $\{\text{Cu}_2(\text{BDC})_2\}_n$ ribbon as shown in Fig. 2a. The **L** ligands display a μ_2 -bridging coordinated mode (*via* ligation of the pyridyl nitrogen atoms). The dihedral angle between the pyridyl rings is 1.78°. The **L** ligands connect the Cu(II) ions belonging to adjacent

$\{\text{Cu}_2(\text{BDC})_2\}_n$ ribbons to form a layer (Fig. 2c). In the layer, the Cu(II) ions are linked by μ_2 -bridging ligands **L** resulting in a $[\text{Cu}-\text{L}]_n$ polymer chain, in which the non-bonding distance Cu...Cu is 18.16 Å (Fig. 2b).

Each Cu(II) ion is surrounded by two **L** and three BDC ligands, and thus can be defined as a 5-connected node. Each BDC links three metal Cu(II) ions, and is to be regarded as a 3-connected node. The **L** ligand associated with two 5-connected Cu(II) ions serves as a simple linear linker. Thus the 2D structure of complex **1** is best described as a (3,5)-connected network with $\{4^2.6^7.8\}\{4^2.6\}$ topology, as shown in Fig. 2d. Moreover, the layers of **1** are extended to a 3D supramolecular frameworks by two types of hydrogen bonding interactions [N–H...O: N3...O5 = 3.339(7), C–H...O: C26...O5 = 3.220(5) Å], as shown in Fig. 3.

Crystal and molecular structure of $[\text{Cu}_2(\text{L})_{0.5}(\text{SIP})(\text{OH})(\text{H}_2\text{O})]\cdot 2\text{H}_2\text{O}$ (**2**)

X-Ray diffraction analysis has revealed that complex **2** is a 3D supramolecular network based on coordination polymeric layers formed by tetranuclear copper clusters $[\text{Cu}_4(\mu_3-\text{OH})_2(\text{H}_2\text{O})_2(\text{O}_2\text{C})_4]$, ligands **L** with μ_6 -bridging mode and SIP anions. As shown in Fig. 4, the fundamental building unit is composed of two crystallographical independent Cu(II) ions (Cu1, Cu2). Cu1 is six-coordinated by two oxygen atoms from the carboxyl groups of two SIP ligands with distances of 1.971(2) (Cu1–O3) and 1.982(3) Å (Cu1–O7#1), one oxygen atom from a coordinated water molecule (Cu1–O2 2.285(2) Å), one oxygen atom from a carbonyl group of **L** (Cu1–O1 2.542(3) Å), one hydroxyl oxygen atom O5#1 (Cu1–O5#1 1.980(2) Å), and one nitrogen atom from a pyridyl group (Cu1–N1 2.045(3) Å), showing a distorted octahedral geometry. The other Cu(II) ion (Cu2) is five-coordinated by two oxygen atoms belonging to two SIP ligands (Cu2–O4 1.922(3), Cu2–O6 1.933(2) Å), two hydroxyl oxygen atoms with the distances 1.961(2) (Cu2–O5)

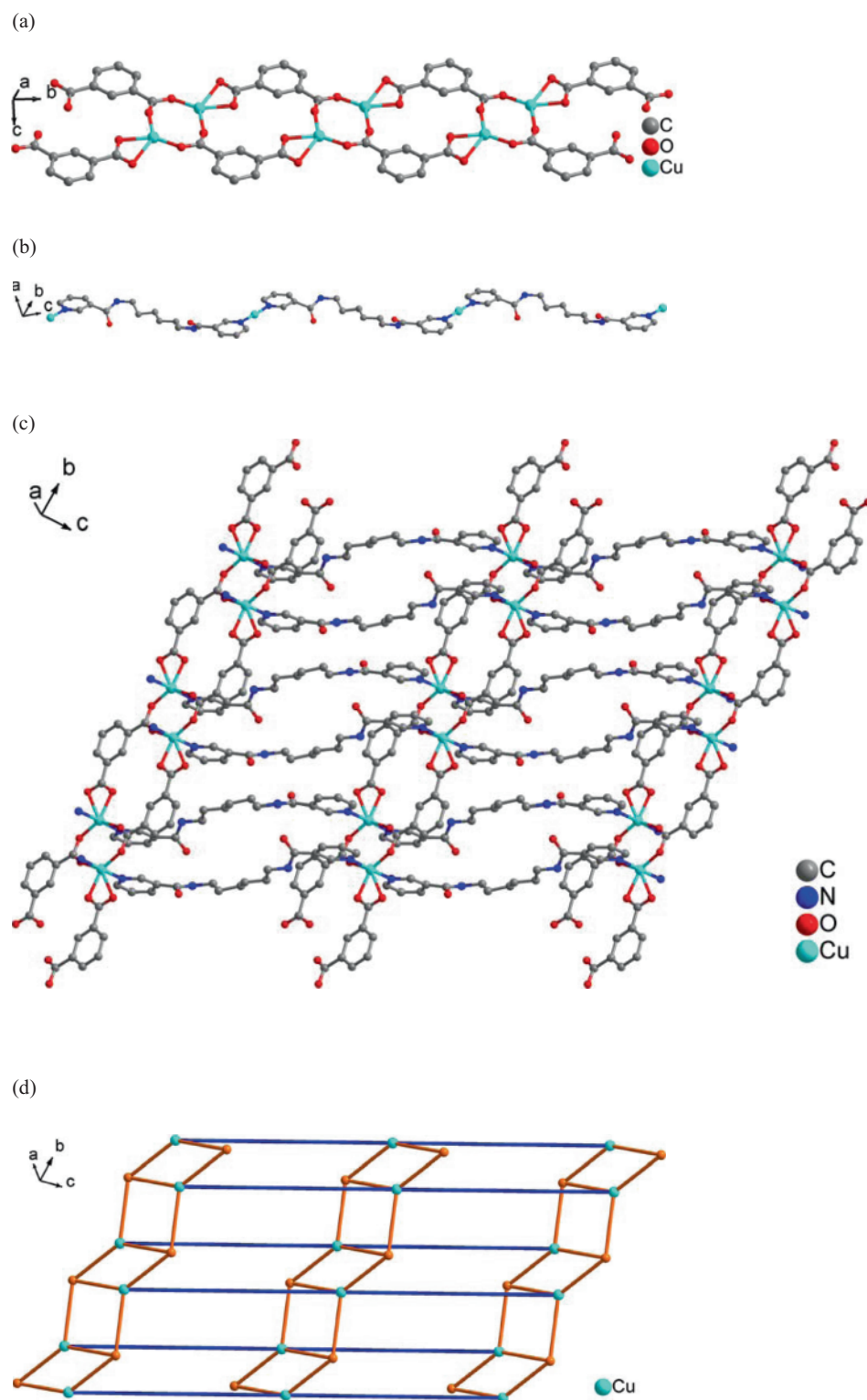


Fig. 2 (color online). (a) The neutral $\{Cu_2(BDC)_2\}_n$ ribbon-like chain formed by the BDC ligand in complex **1**; (b) the $[Cu-L-Cu]$ polymer chain formed by the L ligand; (c) the polymeric layer of **1** formed by BDC and L ligands; (d) the schematic network in **1** (orange ball and line: BDC ligands; blue line: L ligands).

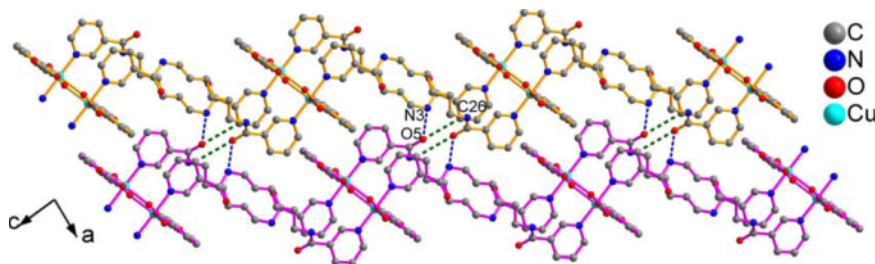


Fig. 3 (color online). The 3D supramolecular framework of complex **1** formed by hydrogen bonding interactions [hydrogen bonds: blue dotted line, N3...O5; green dotted line, O5...C28].

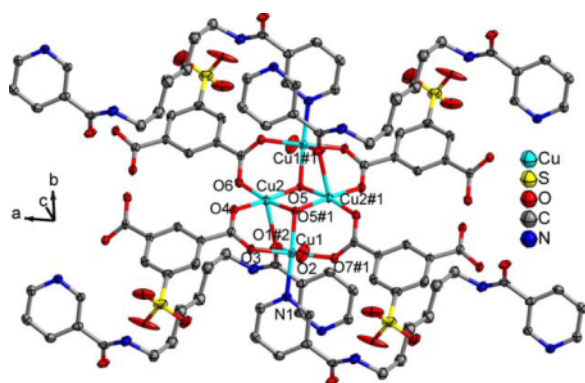


Fig. 4 (color online). The coordination environment of the Cu(II) ions in complex **2** (ellipsoids at the 50% probability level). All H atoms and solvent water molecules are omitted for clarity.

and 1.975(2) Å (Cu2–O5#1), and one carbonyl oxygen atom from a L ligand (Cu1–O1#2 2.323(2) Å) to complete a distorted tetragonal pyramidal geometry.

The Cu1 and Cu2 ions are connected by four carboxylic groups with bidentate coordination fashion to form a tetranuclear copper cluster $[\text{Cu}_4(\mu_3\text{-OH})_2(\text{H}_2\text{O})_2(\text{O}_2\text{C-})_4]$, as shown in Fig. 5a. The Cu–O_{hydroxy} bond lengths are within the normal range [20, 21], and the non-bonding Cu...Cu separations are 5.860 Å (Cu(1)···Cu(1)#1), 3.355 Å (Cu(1)···Cu(2)#1), 3.194 Å (Cu(1)···Cu(2)), and 2.929 Å (Cu(2)–Cu(2)#3), which is slightly different from those of 5.938, 3.471, 3.202, and 3.056 Å in a related tetranuclear copper cluster previously reported [22].

The tetranuclear clusters are connected into neutral $[\text{Cu}_4(\text{OH})_2(\text{SIP})_2]_n$ ribbons (Fig. 5a) through bridging SIP ligands with a bis(bidentate) bridging mode of the carboxyl groups. These ribbons are linked by the flexible ligand L to form a layer. The L ligand displays a μ_6 -bridging coordinated mode [each oxygen atom of a carbonyl group coordinated to two different Cu(II) ions, and each nitrogen atom of a pyridine group coordinated to one Cu(II) ion], which is different from that of L in complex **1**. To the best of our knowledge, the μ_6 -bridging coordinated mode has not been reported in other complexes containing bis-pyridyl-bis-amide ligands [23–28]. It thus represents the highest number of metal ions bridged by bis-pyridyl-bis-amide ligands. Ignoring the connection of the SIP ligands, these adjacent Cu(II) ions are linked by the μ_6 -bridging L ligands and μ_3 -bridging hydroxyl oxygen atoms to form a coordination polymeric layer, as shown in Fig. 5b. The two pyridyl rings in complex **2** are parallel with the dihedral angle at 0°.

In order to simplify the 2D network of complex **2**, the $[\text{Cu}_4(\mu_3\text{-OH})_2(\text{H}_2\text{O})_2(\text{O}_2\text{C-})_4]$ tetranuclear clusters and the SIP and L ligands can be considered as connecting nodes or linkers. Each $[\text{Cu}_4(\mu_3\text{-OH})_2(\text{H}_2\text{O})_2(\text{O}_2\text{C-})_4]$ tetranuclear cluster is surrounded by four SIP ligands and four L ligands, acting as an 8-connected node. Each L ligand serves as a 4-connected node, joining together four adjacent tetranuclear clusters (*via* two pyridyl nitrogen atoms and two carbonyl oxygen atoms). The SIP unit connecting with two 8-connected tetranuclear clusters serves as a “V”-shaped linker. The overall topology of the 2D network for complex **2** is best described as a 4,8-connected $\{4^{14}, 6^{10}, 8^4\}\{4^4, 6^2\}$ topology (Fig. 5c). Figure 6 shows that a 3D supramolecular network is generated *via* interlayer C–H...O hydrogen bonding interactions. The carbon atom C13 of SIP and the oxygen atom O2 of coordinated water molecules connect these adjacent polymeric layers through the hydrogen bonding interactions with a C13–H13A...O2 distance of 3.257(5) Å.

IR spectra

The IR spectra of **1** and **2** are consistent with the structural characteristics as determined by single crystal diffraction. The typical stretching bands of carboxy-

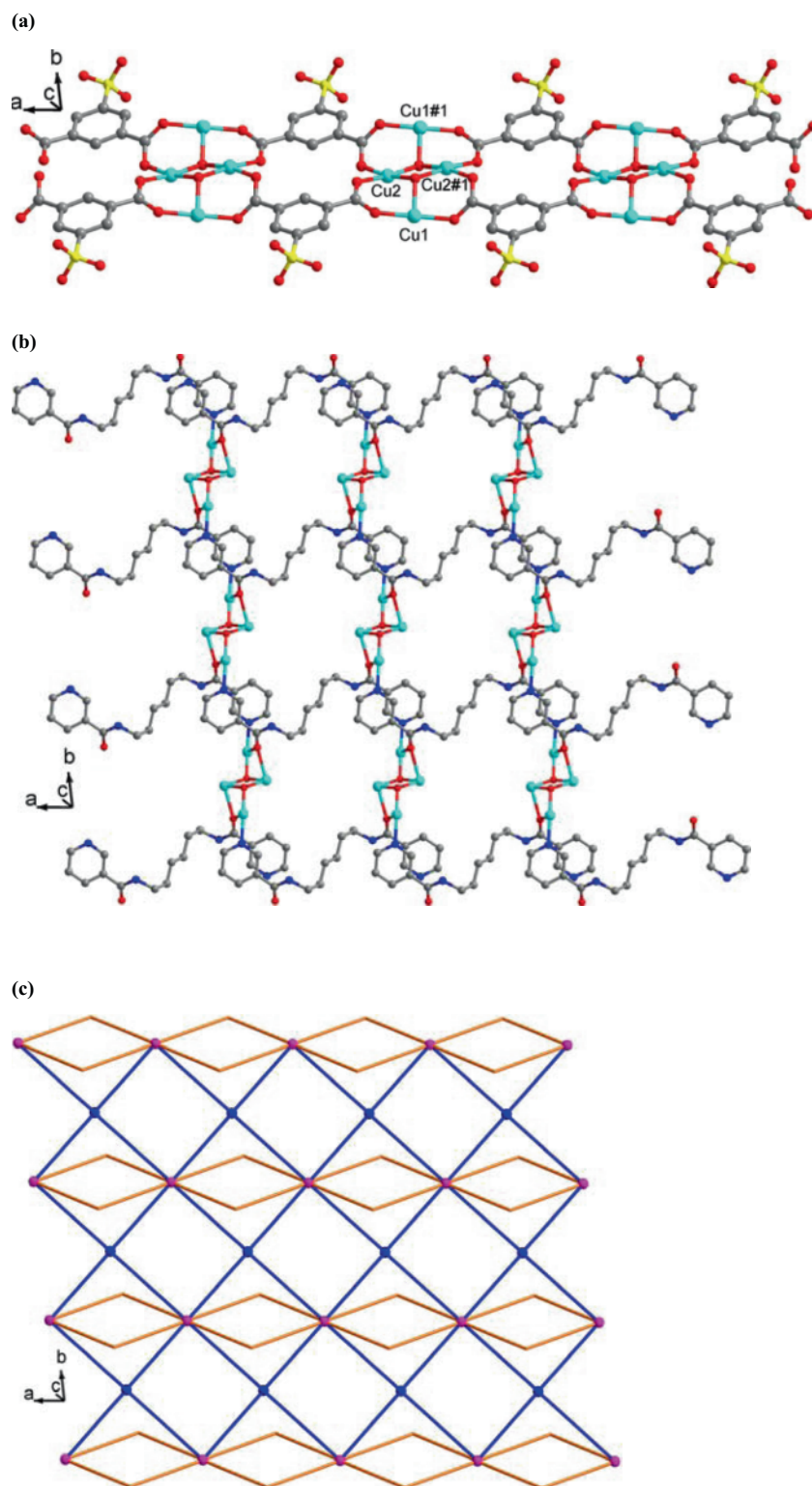


Fig. 5 (color online). (a) The neutral $[\text{Cu}_4(\text{OH})_2(\text{SIP})_2]_n$ ribbon of complex **1**; (b) the polymeric layer formed by L ligands and hydroxyl oxygen atoms; (c) the schematic layer in **2** (the color of balls and lines: pink balls, 8-connected tetranuclear copper clusters; orange lines, 'V'-shaped linker SIP; blue balls and lines, 4-connected L ligands).

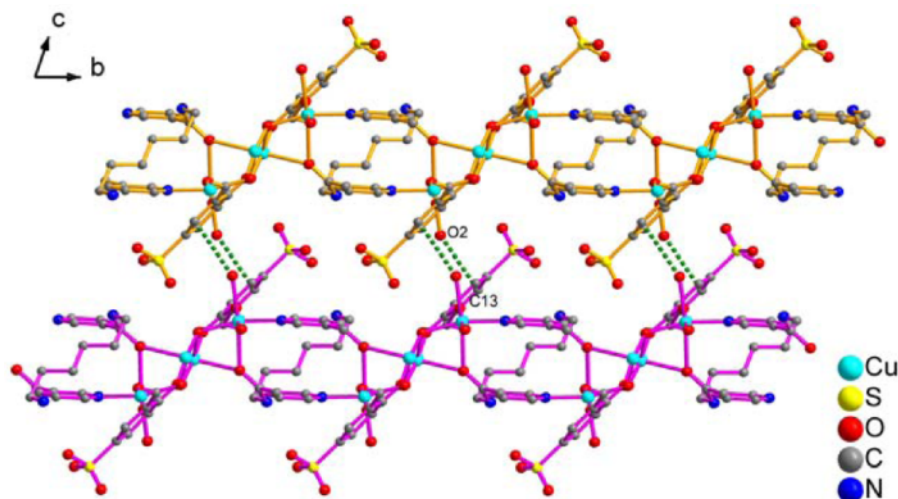


Fig. 6 (color online). The 3D supramolecular framework of complex **2** formed by hydrogen bonding interactions [hydrogen bond: green dotted line, C13...O2].

late groups from the BDC ligands appear at 1358 and 1615 cm^{-1} for complex **1**. Asymmetric and symmetric C–O stretching modes of the carboxylate groups of the completely deprotonated SIP ligands correspond to the strong features at 1378 and 1603 cm^{-1} for complex **2**. The presence of the sulfonate groups can be corroborated by strong S–O stretching vibrations 1444 cm^{-1} for **2**. Weak absorptions in the region of 3040 to 3420 cm^{-1} for **1**, and 3088 to 3400 cm^{-1} for **2**, can be attributed to $\nu_{\text{N-H}}$ of the ligand L. The strong broad band at around 3433 cm^{-1} for **1** and 3450 cm^{-1} for **2** is assigned to the vibrations of hydroxyl groups from water molecules.

Thermal properties

To examine the thermal stability of the title complexes, thermogravimetric (TG) analyses were carried out in the temperature range of 30–600 °C (Fig. 7). The TG curves of complexes **1** and **2** exhibit two weight loss steps. For complex **1**, the first step from 80 to 140 °C is attributed to the loss of the lattice water molecules. The weight loss is about 3.8%, corresponding to the calculated value of 3.2%. For complex **2**, the continuous weight loss from 85 to 210 °C is attributed to the loss of the lattice water and coordinated water molecules. This weight loss is about 8.5%, in correspondence with the calculated value of 8.9%. The second sharp weight loss was observed beginning at about 260 °C for **1** and 280 °C for **2**, which can be ascribed to the decomposition of the organic ligands. The

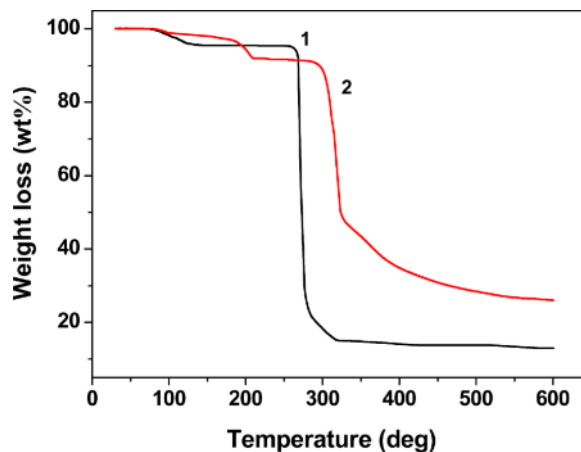


Fig. 7 (color online). Thermogravimetric curves of **1** and **2**.

remaining weights (13.4% for **1**, 26.3% for **2**) correspond to the percentage (13.9% for **1**, 26.5% for **2**) of CuO [29]. For compound **1**, the second weight loss in a very narrow temperature range might be attributed to the fast decarboxylation process. Compound **2** requires high temperatures that may be caused by the presence of sulfonate groups.

Electrochemical behavior of 1-CPE and 2-CPE

To study their electrochemical behavior, carbon paste electrodes bulk-modified with complexes **1** and **2** (**1**-CPE and **2**-CPE) were fabricated as the working electrodes due to the insolubility of the two com-

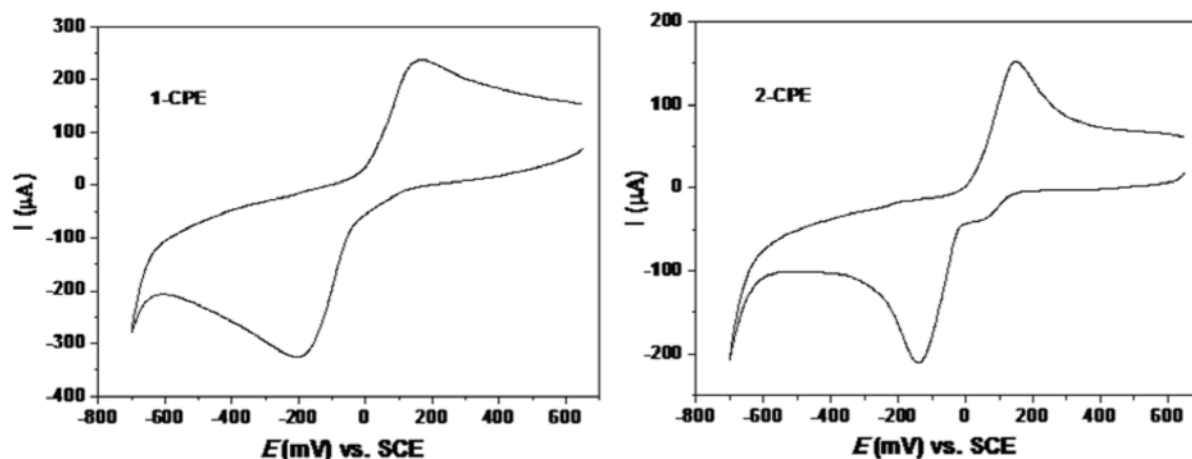


Fig. 8. Cyclic voltammograms of title complexes bulk-modified carbon paste electrodes (**1-CPE** and **2-CPE**) in 1 M H₂SO₄ aqueous solution in the potential range of 600 to –700 mV (scan rate: 80 mV s^{–1}).

plexes. Compared with other film-modified electrodes, the bulk-modified CPEs show long-term stability and especially good surface renewability by simple mechanical polishing in the event of surface fouling, which is important in practical application [30]. The cyclic voltammograms of the **1-CPE** and **2-CPE** were obtained in 1 M H₂SO₄ aqueous solution, as shown in Fig. 8. In the potential range from 600 to –700 mV, a redox couple was observed which should be ascribed to Cu(II)/Cu(I) [30, 31]. The mean peak potentials $E_{1/2} = (E_{pa} + E_{pc})/2$ were –18 mV for **1-CPE**, and 7 mV for **2-CPE**. The electrochemical behavior of **1-CPE** and **2-CPE** is thus similar to that of other reported copper(II) complexes [18, 19]. The slight difference of peak potentials for **1-CPE** and **2-CPE** can be attributed to the different structures of the two copper(II) complexes.

Conclusion

In summary, two new copper(II) coordination polymers constructed from the flexible bis-pyridyl-bis-amide ligand **L** and aromatic polycarboxylate ligands H₂BDC or H₃SIP have been synthesized hydrothermally. The compounds display layer structures with different topologies. The different coordination modes of the **L** ligand play an important role in governing the coordination motifs and the final structures. CPEs bulk-modified with the two insoluble copper(II) complexes show good stability in 1 M H₂SO₄ aqueous solution, and thus may be used as

Table 1. Crystal data and structure refinement for complexes **1** and **2**.

| Formula | C ₂₆ H ₂₈ CuN ₄ O ₇ | C ₁₇ H ₂₁ Cu ₂ N ₂ O ₁₂ S |
|---|---|--|
| Formula wt. | 572.07 | 604.51 |
| Crystal size, mm ³ | 0.21 × 0.16 × 0.14 | 0.16 × 0.14 × 0.12 |
| Crystal system | triclinic | triclinic |
| Space group | <i>P</i> $\bar{1}$ | <i>P</i> $\bar{1}$ |
| <i>T</i> , K | 293(2) | 293(2) |
| <i>a</i> , Å | 9.460(5) | 10.6562(9) |
| <i>b</i> , Å | 10.020(5) | 10.7128(9) |
| <i>c</i> , Å | 14.017(5) | 11.1145(10) |
| α , deg | 87.754(5) | 70.2720(10) |
| β , deg | 84.017(5) | 68.8180(10) |
| γ , deg | 77.789(5) | 82.9120(10) |
| <i>V</i> , Å ³ | 1291.3(10) | 1113.64(17) |
| <i>Z</i> | 2 | 2 |
| <i>D</i> _{calcd} , g cm ^{–3} | 1.47 | 1.78 |
| μ (Mo <i>K</i> α), mm ^{–1} | 0.9 | 2.1 |
| <i>F</i> (000), e | 594 | 600 |
| <i>hkl</i> range | –11 ≤ <i>h</i> ≤ +11 –8 ≤ <i>k</i> ≤ +11 –16 ≤ <i>l</i> ≤ +16 | –12 ≤ <i>h</i> ≤ +13 –9 ≤ <i>k</i> ≤ +13 –12 ≤ <i>l</i> ≤ +13 |
| θ_{max} , deg | 25.00 | 26.00 |
| Refl. collected/ unique/ <i>R</i> _{int} | 17 401/ 4489/0.0385 | 6418/ 4324/0.0141 |
| Refl. “observed” with <i>I</i> > 2 σ (<i>I</i>) | 4034 | 3741 |
| <i>R</i> ₁ [<i>I</i> > 2 σ (<i>I</i>)]/ <i>wR</i> ₂ (all data) | 0.0440/0.1054 | 0.0388/0.1100 |
| $\Delta\rho_{fin}$ (max/min), e Å ^{–3} | 1.34/–1.37 | 1.65/–0.81 |

electrode materials. Further studies on metal-organic complexes with this flexible bis-pyridyl-bis-amide ligand and its analogs are underway in our laboratory.

| 1 | | | | Table 2. Selected bond lengths (Å) and angles (deg) for complexes 1 and 2 . |
|--|------------|---------------------|------------|---|
| Cu(1)–O(2) | 2.081(2) | Cu(1)–O(4)#2 | 1.960(2) | |
| Cu(1)–O(1) | 2.533(3) | Cu(1)–N(1) | 2.011(3) | |
| Cu(1)–O(3)#1 | 2.232(2) | Cu(1)–N(4) | 2.016(3) | |
| O(4)#2–Cu(1)–N(1) | 88.80(10) | O(4)#2–Cu(1)–N(4) | 89.80(10) | |
| N(1)–Cu(1)–N(4) | 177.75(11) | O(4)#2–Cu(1)–O(2) | 146.41(9) | |
| N(1)–Cu(1)–O(2) | 90.88(10) | N(4)–Cu(1)–O(2) | 91.26(10) | |
| O(4)#2–Cu(1)–O(3)#1 | 126.95(9) | N(1)–Cu(1)–O(3)#1 | 89.21(10) | |
| N(4)–Cu(1)–O(3)#1 | 90.23(10) | O(2)–Cu(1)–O(3)#1 | 86.62(8) | |
| O(4)#2–Cu(1)–O(1) | 90.10(9) | N(1)–Cu(1)–O(1) | 93.63(10) | |
| N(4)–Cu(1)–O(1) | 88.12(10) | O(2)–Cu(1)–O(1) | 56.40(8) | |
| Symmetry code for 1 : #1 $-x, -y+2, -z$; #2 $x, y-1, z$ | | | | |
| 2 | | | | |
| Cu(1)–O(3) | 1.971(2) | Cu(2)–O(4) | 1.922(3) | |
| Cu(1)–O(5)#1 | 1.980(2) | Cu(2)–O(6) | 1.933(2) | |
| Cu(1)–O(7)#1 | 1.982(3) | Cu(2)–O(5) | 1.961(2) | |
| Cu(1)–N(1) | 2.045(3) | Cu(2)–O(5)#1 | 1.975(2) | |
| Cu(1)–O(2) | 2.285(4) | Cu(2)–O(1)#2 | 2.323(2) | |
| Cu(1)–O(1)#2 | 2.542(3) | | | |
| O(3)–Cu(1)–O(5)#1 | 91.06(10) | O(4)–Cu(2)–O(6) | 87.26(11) | |
| O(3)–Cu(1)–O(7)#1 | 172.14(12) | O(4)–Cu(2)–O(5) | 173.84(11) | |
| O(5)#1–Cu(1)–O(7)#1 | 91.43(10) | O(6)–Cu(2)–O(5) | 93.81(10) | |
| O(3)–Cu(1)–N(1) | 90.23(11) | O(4)–Cu(2)–O(5)#1 | 93.95(10) | |
| O(5)#1–Cu(1)–N(1) | 164.70(11) | O(6)–Cu(2)–O(5)#1 | 169.06(10) | |
| O(7)#1–Cu(1)–N(1) | 89.34(11) | O(5)–Cu(2)–O(5)#1 | 83.85(10) | |
| O(3)–Cu(1)–O(2) | 88.26(13) | O(4)–Cu(2)–O(1)#2 | 96.76(11) | |
| O(5)#1–Cu(1)–O(2) | 97.95(15) | O(6)–Cu(2)–O(1)#2 | 108.90(10) | |
| O(7)#1–Cu(1)–O(2) | 84.01(14) | O(5)–Cu(2)–O(1)#2 | 88.65(10) | |
| N(1)–Cu(1)–O(2) | 97.33(16) | O(5)#1–Cu(2)–O(1)#2 | 81.79(9) | |
| O(3)–Cu(1)–O(5)#1 | 91.06(10) | O(4)–Cu(2)–O(6) | 87.26(11) | |
| Symmetry code for 2 : #1 $-x, -y+1, -z$; #2 $-x, -y, -z$ | | | | |

Experimental Section

Materials and methods

All reagents employed were commercially available and used as received without further purification. **L** was synthesized by the literature method [32, 33]. FT-IR spectra (KBr pellets) were taken on a Magna FT-IR 560 spectrometer, and the elemental analyses (C, H, and N) were carried out on a Perkin-Elmer 2400 CHN elemental analyzer. Thermogravimetric analysis was carried out with a Pyris Diamond TG-DTA instrument. The electrochemical experiments were performed using a CHI 440 electrochemical quartz crystal microbalance. A conventional three-electrode cell was used at room temperature. The CPEs bulk-modified with the title complexes (**1**-CPE and **2**-CPE) were used as working electrodes. An SCE and a platinum wire were employed as reference and auxiliary electrodes, respectively.

Synthesis of $[Cu(L)(BDC)] \cdot H_2O$ (**1**)

A mixture of $CuCl_2 \cdot 2H_2O$ (0.051 g, 0.3 mmol), H_2BDC (0.025 g, 0.15 mmol), **L** (0.033 g, 0.1 mmol), H_2O (12 mL), and NaOH (0.014 g, 0.35 mmol) was stirred for 30 min in air,

then transferred and sealed in a 25 mL Teflon reactor, which was heated at 120 °C for 6 d, leading to the formation of blue block-shaped crystals of **1**, which were washed with water and dried in air. Yield: ~ 31 % (based on Cu). – Anal. for $C_{26}H_{28}CuN_4O_7$: calcd. C 54.54, H 4.93, N 9.79; found C 54.44, H 4.85, N 9.88. – IR (KBr, cm^{-1}): $\nu = 3433$ s, 3420 w, 3305 w, 3240 w, 3102 w, 3040 w, 2946 m, 2862 w, 2359 m, 2335 w, 1645 s, 1615 s, 1538 w, 1502 w, 1419 s, 1358 w, 1322 m, 1287 m, 1262 s, 1217 s, 1149 m, 1062 w, 1036 w, 1005 s, 908 w, 848 s, 759 s, 718 m, 668 m, 632 s, 608 w, 533 m.

Synthesis of $[Cu_2(L)_{0.5}(SIP)(OH)(H_2O)] \cdot 2H_2O$ (**2**)

The synthesis method of **2** was similar to that for **1** except for ligand H_3SIP (0.040 g, 0.16 mmol) as the substitute of H_2BDC , and the different amount of NaOH (0.0152 g, 0.38 mmol) added to adjust the pH. Yield: ~ 25 % (based on Cu). – Anal. for $C_{17}H_{21}Cu_2N_2O_{12}S$: calcd. C 33.75, H 3.50, N 4.63; found C 33.84, H 3.40, N 4.52. – IR (KBr, cm^{-1}): $\nu = 3454$ s, 3400 w, 3340 m, 3281 w, 3234 w, 3128 w, 3088 w, 2764 w, 2518 m, 2472 w, 2359 s, 2253 w, 2167 w, 2100 w, 2027 w, 1941 w, 1776 m, 1696 m, 1603 s, 1550 s, 1444

s, 1378 s, 1318 m, 1258 w, 1193 s, 1099 w, 1053 m, 974 m, 867 m, 814 w, 781 m, 735 s, 681 s, 629 s, 582 s.

Crystal structure determinations

Crystallographic data for the title compounds were collected on a Bruker Smart 1000 CCD diffractometer with MoK α radiation ($\lambda = 0.71073$ Å) in ω scan mode in the range of $2.08 \leq \theta \leq 25.00^\circ$ for **1** and $2.05 \leq \theta \leq 26.00^\circ$ for **2**. The structures were solved by Direct Methods using the program SHELXS of the SHELXTL package and refined by full-matrix least-squares methods with SHELXL [34, 35]. The atoms C15, C16, C18, and O6 of complex **1** were found to be disordered and refined in a split-atom model. All non-hydrogen atoms were refined anisotropically, and all hydrogen atoms were placed in geometrically idealized positions and refined isotropically with fixed displacement factors. The OH hydrogen atoms in **2** could not be found in difference

density syntheses but were included in the final molecular formula, which has also been done in similar metal-organic complexes previously reported [19]. A summary of crystal data and structure refinements for the two complexes is provided in Table 1. Selected bond lengths and angles of the title complexes are listed in Table 2.

CCDC 885865 (**1**) and 887509 (**2**) contain the supplementary crystallographic data for this paper. These data can be obtained free of charge from The Cambridge Crystallographic Data Centre via www.ccdc.cam.ac.uk/data_request/cif.

Acknowledgement

The supports of the National Natural Science Foundation of China (no. 20871022 and 21171025), New Century Excellent Talents in University (NCET-09-0853), and the Natural Science Foundation of Liaoning Province (no. 201102003 and 2009402007) are gratefully acknowledged.

- [1] M. D. Allendorf, C. A. Bauer, R. K. Bhakta, R. J. T. Houk, *Chem. Soc. Rev.* **2009**, 38, 1330–1352.
- [2] F. Blank, C. Janiak, *Coord. Chem. Rev.* **2009**, 253, 827–861.
- [3] K. C. Cheung, W. L. Wong, D. L. Ma, T. S. Lai, K. Y. Wong, *Coord. Chem. Rev.* **2007**, 251, 2367–2385.
- [4] J. P. Zhang, X. C. Huang, X. M. Chen, 2009, *Chem. Soc. Rev.* **2009**, 38, 2385–2396.
- [5] Z. B. Han, M. Y. Zhang, D. Q. Yuan, S. Fu, G. X. Zhang, X. F. Wang, *CrystEngComm* **2011**, 13, 6945–6949.
- [6] Q. Y. Liu, D. Q. Yuan, L. Xu, *Cryst. Growth Des.* **2007**, 7, 1832–1843.
- [7] X. Li, R. Cao, W. Bi, D. Yuan, D. Sun, *Eur. J. Inorg. Chem.* **2005**, 3156–3166.
- [8] Y. J. Song, H. Kwak, Y. M. Lee, S. H. Kim, S. H. Lee, B. K. Park, J. Y. Jun, S. M. Yu, C. Kim, S. J. Kim, Y. Kim, *Polyhedron* **2009**, 28, 1241–1252.
- [9] C. P. Li, Q. Yu, J. Chen, M. Du, *Cryst. Growth Des.* **2010**, 10, 2650–2660.
- [10] X. L. Wang, J. Li, H. Y. Lin, H. L. Hu, B. K. Chen, B. Mu, *Solid State Sci.* **2009**, 11, 2118–2124.
- [11] H. Wang, M. X. Li, M. Shao, Z. X. Wang, *J. Mol. Struct.* **2008**, 889, 154–159.
- [12] M. Du, Z. H. Zhang, X. J. Zhao, H. Cai, *Cryst. Growth Des.* **2006**, 6, 114–121.
- [13] L. Rajput, K. Biradha, *Polyhedron* **2008**, 27, 1248–1255.
- [14] Y. Gong, J. Li, J. B. Qin, T. Wu, R. Cao, J. H. Li, *Cryst. Growth Des.* **2011**, 11, 1662–1674.
- [15] C. Y. Wang, Z. M. Wilseck, R. M. Supkowski, R. L. LaDuca, *CrystEngComm* **2011**, 13, 1391–1399.
- [16] J. S. Lucas, A. L. Pochodylo, R. L. LaDuca, *CrystEngComm* **2010**, 12, 3310–3317.
- [17] X. L. Wang, B. Mu, H. Y. Lin, G. C. Liu, A. X. Tian, S. Yang, *CrystEngComm* **2012**, 14, 1001–1009.
- [18] X. L. Wang, H. Y. Lin, B. Mu, A. X. Tian, G. C. Liu, *Dalton Trans.* **2010**, 39, 6187–6189.
- [19] X. L. Wang, H. Y. Lin, B. Mu, A. X. Tian, G. C. Liu, N. H. Hu, *CrystEngComm* **2011**, 13, 1990–1997.
- [20] S. Hikichi, M. Yoshizawa, Y. Sasajura, M. Ajita, Y. Morroja, *J. Am. Chem. Soc.* **1998**, 120, 10567.
- [21] C. M. Liu, D. Q. Zhang, D. B. Zhu, *Cryst. Growth Des.* **2003**, 3, 363–368.
- [22] W. X. Chen, S. T. Wu, L. S. Long, R. B. Huang, L. S. Zheng, *Cryst. Growth Des.* **2007**, 7, 1171–1175.
- [23] D. K. Kumar, A. Das, P. Dastidar, *CrystEngComm* **2007**, 9, 548–555.
- [24] N. N. Adarsh, D. K. Kumar, P. Dastidar, *CrystEngComm* **2008**, 10, 1565–1573.
- [25] Y. Gong, Y. C. Zhou, T. F. Liu, J. Lü, D. M. Proserpio, R. Cao, *Chem. Commun.* **2011**, 47, 5982–5984.
- [26] G. M. Sun, Y. M. Song, Y. Liu, X. Z. Tian, H. X. Huang, Y. Zhu, Z. J. Yuan, X. F. Feng, M. B. Luo, S. J. Liu, W. Y. Xu, F. Luo, *CrystEngComm* **2012**, 14, 5714–5716.
- [27] Y.-F. Hsu, H.-L. Hu, C.-J. Wu, C.-W. Yeh, D. M. Proserpio, J.-D. Chen, *CrystEngComm* **2009**, 11, 168–176.
- [28] S. Hasegawa, S. Horike, R. Matsuda, S. Furukawa, K. Mochizuki, Y. Kinoshita, S. Kitagawa, *J. Am. Chem. Soc.* **2007**, 129, 2607–2614.
- [29] V. Amendola, L. Fabbri, F. Foti, M. Licchelli, C. Mangano, P. Pallavicini, A. Poggi, D. Sacchi,

- A. Taglietti, *Coord. Chem. Rev.* **2006**, 250, 273–299.
- [30] X. L. Wang, H. Y. Zhao, H. Y. Lin, G. C. Liu, J. N. Fang, B. K. Chen, *Electroanalysis* **2008**, 20, 1055–1060.
- [31] G. G. Gao, L. Xu, W. J. Wang, W. J. An, Y. F. Qiu, Z. Q. Wang, E. B. Wang, *J. Phys. Chem. B* **2005**, 109, 8948–8953.
- [32] S. Muthu, J. H. K. Yip, J. J. Vittal, *J. Chem. Soc., Dalton Trans.* **2001**, 3577–3584.
- [33] S. Muthu, J. H. K. Yip, J. J. Vittal, *J. Chem. Soc., Dalton Trans.* **2002**, 4561–4568.
- [34] G. M. Sheldrick, SHELXS-97, Program for the Solution of Crystal Structures, University of Göttingen, Göttingen (Germany) **1997**. See also: G. M. Sheldrick, *Acta Crystallogr.* **1990**, A46, 467–473.
- [35] G. M. Sheldrick, SHELXL-97, Program for the Refinement of Crystal Structures, University of Göttingen, Göttingen (Germany) **1997**. See also: G. M. Sheldrick, *Acta Crystallogr.* **2008**, A64, 112–122.